Semiclassical Statistical Mechanics*

C. A. A. de Carvalho†
Instituto de Física, Universidade Federal do Rio de Janeiro,
Cx. Postal 68528, CEP 21945-970, Rio de Janeiro, RJ, Brasil

R. M. Cavalcanti‡
Departamento de Física, Pontifícia Universidade Católica do Rio de Janeiro,
Cx. Postal 38071, CEP 22452-970, Rio de Janeiro, RJ, Brasil

Abstract

We use a semiclassical approximation to derive the partition function for an arbitrary potential in one-dimensional Quantum Statistical Mechanics, which we view as an example of finite temperature scalar Field Theory at a point. We rely on Catastrophe Theory to analyze the pattern of extrema of the corresponding path-integral. We exhibit the propagator in the background of the different extrema and use it to compute the fluctuation determinant and to develop a (nonperturbative) semiclassical expansion which allows for the calculation of correlation functions. We discuss the examples of the single and double-well quartic anharmonic oscillators, and the implications of our results for higher dimensions.

---

*Invited talk at the La Plata meeting on 'Trends in Theoretical Physics', La Plata, April, 1997

†e-mail: aragao@if.ufrj.br

‡e-mail: rmc@fis.puc-rio.br

I. INTRODUCTION

The development of nonperturbative methods for quantum field theories remains as much a challenge as a necessity. The many areas of Physics where field-theoretic approaches have proved useful are full of examples of phenomena whose description lies outside the scope of perturbation theory. In most cases, a reliable treatment of the nonperturbative dynamics is still lacking.

With the exception of a limited number of exactly solvable models, most systems requiring nonperturbative methods have been the object of approximate treatments. This is an unavoidable consequence of the complexity of the dynamics involved. Nevertheless, it should not prevent us from having a clearer understanding of the physics, as long as we have some control over the approximations made.

The approximate methods most commonly used could, perhaps, be classified into three major groups: expansions around special limits, variational methods and numerical techniques. Semiclassical and $1/N$ expansions, Gaussian and Hartree-Fock methods, and Monte Carlo techniques in lattice calculations exemplify each respective group. In all of them, serious technical difficulties stand in the way of establishing reliable controls and, in some cases, of even fully implementing the approximation scheme.

Semiclassical expansions certainly pose hard problems for both their implementation and control. In this article, we discuss a physical situation where such problems can be overcome: one-dimensional Quantum Statistical Mechanics or, from a field-theoretic point of view, scalar finite temperature Field Theory in zero spatial dimension. The drastic reduction in dimensionality is the price we have to pay to accomplish our goal: a thorough semiclassical treatment whose results can be compared to those of perturbation theory, as well as to exact ones, when available. One should not forget, however, that numerous applications in Physics can be studied within this framework, and that, as we shall indicate in the sequel, symmetries may reduce higher dimensional problems to situations where our results may still be used.

The article will start with a discussion of the quadratic semiclassical approximation (Section II[1]), comprising an analysis of the extrema of the classical action and of the fluctuation determinants around them. A connection to Catastrophe Theory allows for the identification of the minima amidst the complexity of the set of classical solutions. The next step (Section III) is the derivation, using techniques described in [2,3], of the semiclassical propagator in the background of any one of the extrema, a crucial result which leads to the expression for the fluctuation determinant and serves as the basis for a semiclassical expansion (Section IV). The expansion provides, already in first order, nonperturbative estimates for correlation functions. Ground states of quartic anharmonic oscillators can be computed to that order: the result contains a sum over an infinite number of diagrams in perturbation theory, an indication of the power of the technique. Finally (Section V), we summarize our conclusions and comment on possible applications of these results in higher dimensions.

---

[1]This section is strongly based on Ref. [1].

II. THE QUADRATIC SEMICLASSICAL APPROXIMATION

A. Extrema and determinants

The partition function for a one-dimensional quantum-mechanical system in an arbitrary potential, $V(x)$, can be written as a path-integral [4,5]:

$$Z(\beta) = \int_{-\infty}^{\infty} dx_0 \int_{x(0)=x_0}^{x(\beta\hbar)=x_0} [Dx(\tau)]\, \mathrm{e}^{-S/\hbar}\,, \tag{2.1}$$

$$S = \int_0^{\beta\hbar} d\tau\, \left[\frac{1}{2}M\dot{x}^2 + V(x)\right]\,. \tag{2.2}$$

As mentioned before, this can be viewed as the partition function for a scalar finite temperature field theory, in the limiting case where the number of space dimensions is zero.

We may expand the Euclidean action around its minima, i.e., the stable classical trajectories,[2] and keep terms only up to quadratic. The functional integral over the paths can, then, be performed to yield a quadratic semiclassical evaluation of (2.1):

$$Z_{\rm sc}(\beta) = \int_{-\infty}^{\infty} dx_0 \sum_{j=1}^{N(x_0,\beta)} \mathrm{e}^{-S_j(x_0,\beta)/\hbar} \Delta_j^{-1/2}(x_0,\beta)\,, \tag{2.3}$$

where $S_j(x_0,\beta)$ denotes the action and $\Delta_j(x_0,\beta)$ represents the determinant of the fluctuation operator,

$$\hat{F}_j = -M\frac{d^2}{d\tau^2} + V''[x_j(\tau)]\,, \tag{2.4}$$

both calculated at the j-th classical trajectory, $x_j(\tau)$, satisfying the boundary conditions $x_j(0) = x_j(\beta\hbar) = x_0$; $N(x_0,\beta)$ is the number of classical trajectories which are minima of the action functional.

The action has a simple expression in terms of the turning points of the classical trajectory:

$$S_j(x_0,\beta) = \beta\hbar\, V(x_\pm^j) \pm 2\int_{x_0}^{x_\pm^j} dx\, Mv(x,x_\pm^j) + 2n\int_{x_-^j}^{x_+^j} dx\, Mv(x,x_\pm^j)\,. \tag{2.5}$$

Here, $v(x,y) \equiv \sqrt{(2/M)[V(x)-V(y)]}$ and x_+^j (x_-^j) are turning points to the right (left) of x_0. The first term in (2.5) corresponds to the high-temperature limit of $Z(\beta)$, where the classical paths collapse to a point, i.e., $x_\pm^j \to x_0$. For motion in regions where the inverted potential is unbounded (hereafter called unbounded motion), $n = 0$. For periodic motion, n counts the number of periods and the second term is absent. For bounded aperiodic motion, all terms are present. The last two terms will be negligible for potentials which vary little

---

[2]For classical trajectories we mean solutions of the Euler-Lagrange equation $M\ddot{x} - V'(x) = 0$, which is the equation of motion for a particle moving in the potential *minus* V.

over a thermal wavelength, $\lambda = \hbar\sqrt{\beta/M}$. However, by decreasing the temperature, quantum effects become important.

For trajectories having a single turning point ($n = 0$), $x_\pm^j$ are given implicitly by

$$\beta\hbar = \pm 2 \int_{x_0}^{x_\pm^j} \frac{dx}{v(x, x_\pm^j)}\,, \tag{2.6}$$

and the fluctuation determinant by

$$\Delta_j(x_0, \beta) = \pm \frac{4\pi\hbar^2[V(x_\pm^j) - V(x_0)]}{MV'(x_\pm^j)} \left[\frac{\partial\beta}{\partial x_\pm^j}\right]_{x_0}\,. \tag{2.7}$$

For trajectories with two turning points, we may generalize (2.7) to:

$$\Delta_j(x_0, \beta) = \frac{4\pi\hbar^2[V(x_\pm^j) - V(x_0)]}{M} \left\{ \frac{n_+}{V'(x_+^j)} \left[\frac{\partial\beta}{\partial x_+^j}\right]_{x_0} - \frac{n_-}{V'(x_-^j)} \left[\frac{\partial\beta}{\partial x_-^j}\right]_{x_0} \right\}. \tag{2.8}$$

$n_\pm$ counts the number of visits to the two turning points, $x_\pm^j$. As we shall see in the sequel, trajectories with more than one turning point are naturally excluded from the calculation. The derivations of (2.7) and (2.8) will be outlined in section III.

Formulae (2.5), (2.7) and (2.8) do not require full knowledge of the classical trajectory, as the dependence on $x_j(\tau)$ comes only through the turning point. Furthermore, equations (2.7) and (2.8) yield a direct evaluation of the determinant which bypasses solving an eigenvalue problem for each stable classical trajectory. To see how this can simplify the evaluation of $Z_{\rm sc}(\beta)$, let us take the harmonic oscillator, $V(x) = \frac{1}{2}M\omega^2x^2$, as an example. In this case, given x_0 and β there is only one trajectory, with a single turning point, given by $x_+(x_-) = x_0/\cosh(\beta\hbar\omega/2)$ for $x_0 < 0$ (> 0). S and Δ can also be readily calculated, the final result being

$$Z_{\rm sc}(\beta) = \int_{-\infty}^{\infty} dx_0\, \mathrm{e}^{-(M\omega x_0^2/\hbar)\tanh(\beta\hbar\omega/2)} \sqrt{\frac{M\omega}{2\pi\hbar\sinh(\beta\hbar\omega)}}\,, \tag{2.9}$$

which in this case is exact.

For the single-well quartic anharmonic oscillator, $V(x) = \frac{1}{2}M\omega^2x^2 + \frac{\lambda}{4}x^4$, $\lambda > 0$, it is still true that there is only one trajectory, given x_0 and β, which has a single turning point. Eq. (2.6) yields:

$$x_\pm = x_0\,\mathrm{cn}(u_\pm, k_\pm), \tag{2.10}$$

$$u_\pm = \frac{\beta\hbar\omega}{2}\sqrt{1 + \frac{\lambda x_\pm^2}{M\omega^2}}, \tag{2.11}$$

$$k_\pm^2 = \frac{M\omega^2 + (1/2)\lambda x_\pm^2}{M\omega^2 + \lambda x_\pm^2}, \tag{2.12}$$

where $\mathrm{cn}(u, k)$ is one of the Jacobian elliptic functions [6]. We may, then, use Eqs. (2.5) and (2.7), and change the integration variable in (2.3) from x_0 to $x_\pm$ to obtain $Z_{\rm sc}(\beta)$. The resulting integral can be evaluated numerically.

A more interesting situation occurs in the case of the double-well quartic anharmonic oscillator, $V(x) = \lambda(x^2 - a^2)^2$. For $x^2 > a^2$, only single paths with single turning points exist for fixed x_0 and β. However, there is also a region, $x^2 < a^2$, where the classical motion is bounded and a much richer structure exists [7], one in which more than one classical path may exist for given values of x_0 and β.

In a region of bounded classical motion (a well in $-V$), such as $x^2 < a^2$ for the anharmonic oscillator, the number of classical trajectories changes as the temperature drops. If $0 \leq \beta < \pi/\hbar\omega_m$ (where $\omega_m \equiv \sqrt{-V''(x_m)/M}$ and x_m is a local minimum of $-V$), for every x_0 in this region there is only one closed path, with a single turning point, satisfying the classical equations of motion. For $x_0 < x_m$ ($> x_m$) this path goes to the left (right) and returns to x_0. For $x_0 = x_m$, it sits still at the bottom of the well. It is this single-path regime which goes smoothly into the high-temperature limit.

For $\beta = \pi/\hbar\omega_m$, the solution that sits still at x_m becomes unstable. Its fluctuation operator is that of a harmonic oscillator with $\omega^2 = \omega_m^2$. Its finite temperature determinant is $\Delta(x_m, \beta) = 2\pi\hbar \sin(\beta\hbar\omega_m)/M\omega_m$. This goes through zero at $\beta = \pi/\hbar\omega_m$ and becomes negative for $\beta > \pi/\hbar\omega_m$, thus signaling that $x(\tau) = x_m$ becomes unstable. At the same time, two new classical paths appear, symmetric with respect to x_m, as depicted in Fig. 1. Therefore, at $x_0 = x_m$, we go from a single-path regime to a triple-path regime as we cross $\beta = \pi/\hbar\omega_m$. The two new paths are degenerate minima, whereas the path that sits still at x_m becomes a saddle-point of the action, with a single negative mode.

As β grows beyond $\pi/\hbar\omega_m$, an analogous situation occurs for other values of x_0 inside the well. When the fluctuation determinant around the classical path for a given x_0 vanishes, a new classical path appears. Its single turning point lies opposite, with respect to x_m, to that of the formerly unique path. If β is increased further, this trajectory splits into two, as illustrated in Fig. 2. One is a local minimum of the action, whereas the other is a saddle-point, with only one negative mode. Again, we have transitioned from a single to a triple-path regime. As β grows, the triple-path region spreads out around x_m. The frontiers of that region are defined by the points x_0 such that $(\partial\beta/\partial x_\pm)_{x_0} = 0$, where the expression (2.7) for the determinant vanishes.

The phenomenon just described is an example of catastrophe. It takes place whenever the number of classical trajectories changes, with one or more of them becoming unstable, as we lower the temperature. Conversely, we may say that the phenomenon is characterized by the coalescence of two or more of the classical trajectories, as we increase the temperature. This is akin to the ocurrence of caustics in Optics [8], where light rays play the role of classical trajectories and the action is replaced with the optical distance. In the next subsection, we shall use the mathematics of catastrophes to understand how the set of classical trajectories changes with temperature.

B. Catastrophe Theory

If we use the basis of eigenfunctions of the fluctuation operator around classical paths, and denote by s_1 the coordinate associated with the direction of instability of our example, the action can be viewed as $S = S(s_1, \ldots; x_0, \beta)$, with the dots referring to all others. Catastrophe Theory [8,9] allows us to write down the "normal form", S_N, of this generating

function in the three-dimensional subspace made up by the unstable direction of state space (the set of paths) and the two control variables, β and x_0; it is this subspace which is relevant for the study of the onset of instability. As catastrophes are classified by their codimension in control space, which here is two-dimensional, only those of codimension 1 (the fold) or 2 (the cusp) are generic (i.e., structurally stable). The pattern of extrema then leads to the cusp, whose generating function is

$$S_N(s_1; u_1, v_1) = s_1^4 + u_1 s_1^2 + v_1 s_1 \,, \tag{2.13}$$

where u_1 and v_1, the control parameters, are related to β and x_0, respectively. This catastrophe is defined by

$$\frac{\partial S_N}{\partial s_1} = \frac{\partial^2 S_N}{\partial s_1^2} = 0 \,. \tag{2.14}$$

Eliminating s_1 from these equations, we can draw the bifurcation set in control space (the curve $v_1^2 = -4u_1^3/27$), as well as the pattern of extrema of S_N (Fig. 3). Assuming that u_1 and v_1 are linearly related to $(\beta - \pi/\hbar\omega_m)$ and $(x_0 - x_m)$, respectively, for small values of both, we can also schematically plot the classical action (i.e., the action for classical trajectories) as a function of x_0 for different values of β;[3] see Fig. 4(a,b).

New classical trajectories, accompanied by new catastrophes, will occur as we keep increasing β. From $\beta = 2\pi/\hbar\omega_m$, we start having trajectories with $\dot{x}(0) = 0$, i.e., with one full period. For these, the determinant of fluctuations vanishes because the first, not the second bracket of (2.7) goes trough zero. However, the fluctuation operator around such trajectories already has a negative eigenmode. This follows from the fact that the zero-mode, given by $\dot{x}_{\rm cl}(\tau)$, has a node. Thus, it cannot be the ground-state for the associated Schrödinger problem. This means that a new catastrophe takes place along a second direction in function space.

This new catastrophe is also a cusp. At x_m, as β becomes larger than $2\pi/\hbar\omega_m$, the solution that sits still acquires a second negative eigenvalue — thus becoming unstable along a new direction in function space — and two other solutions appear. They both have a negative eigenvalue along the first direction of instability and a positive eigenvalue along the new direction of instability. If we combine the information from both directions, we find that we go from two minima and a saddle-point with only one negative eigenvalue (hereafter, a one-saddle) to two minima, two one-saddles and one two-saddle. The two one-saddles are degenerate in action and represent time-reversed periodic paths. As β increases

---

[3]This plot can be obtained by exploiting the relation between the cusp and the swallowtail catastrophes. The latter has a generating function whose normal form is $W(s_1; a, b, c) = s_1^5 + a s_1^3 + b s_1^2 + c s_1$, where a, b, c are control variables. The extremum condition is, then, $\partial W/\partial s_1 = 0$. The identifications $S_N \equiv -c/5$, $u_1 \equiv 3a/5$ and $v_1 \equiv 2b/5$ will make the additional condition that defines the swallowtail, $\partial^2 W/\partial s_1^2 = 0$, coincide with the requirement $\partial S_N/\partial s_1 = 0$. (In the jargon of catastrophe theory: the bifurcation set for the swallowtail coincides with the equilibrium hypersurface of the cusp.)

beyond $2\pi/\hbar\omega_m$, the same phenomenon takes place for x_0 around x_m: the one-saddles that already existed for $\beta < 2\pi/\hbar\omega_m$ in the three-path region around x_m become unstable along a second direction, and a five-path region grows around x_m, with two minima, two (periodic, degenerate in action) one-saddles and a two-saddle.

The new cusp can be cast into normal form using the second direction of instability:

$$S_N(s_2; u_2, v_2 = 0) = s_2^4 + u_2 s_2^2 \sim (s_2^2 + \frac{u_2}{2})^2 \,. \tag{2.15}$$

The absence of the linear term in Eq. (2.15) [compare with Eq. (2.13)] reflects the degeneracy in action of the two one-saddles. However, there is another degeneracy: since V does not depend on β, if $x_{\rm cl}(\tau)$ is a solution of the Euler-Lagrange equation, so is $x_{\rm cl}(\tau + \tau_0)$. If $x_{\rm cl}(\tau)$ is periodic, $x_{\rm cl}(\tau + \tau_0)$ describes the same path (and so has the same action), but with another starting point. This can be represented in Eq. (2.15) by the choice $u_2 \propto [(x_0 - x_m)^2 + k(2\pi/\hbar\omega_m - \beta)]$, with $k > 0$. See Fig. 4(c)

As we approach $\beta = 3\pi/\hbar\omega_m$, the situation becomes similar to the one near $\beta = \pi/\hbar\omega_m$. The difference is that we now have to deal with a path with more than one and less than two periods. Near $\beta = 4\pi/\hbar\omega_m$, two-period paths intervene, a situation similar to that at $\beta = 2\pi/\hbar\omega_m$. The pattern which develops [10] is depicted in Fig. 5.

Despite the fact that we keep adding new extrema as we lower the temperature, only two of these are stable (i.e., minima). In a semiclassical approximation in euclidean time, appropriate to equilibrium situations, these are the only extrema we have to sum over, meaning that $N(x_0, \beta)$ never exceeds two. For $\beta > \pi/\hbar\omega_m$, there will be regions with either one or two minima of the classical action. The transition from a single-minimum to a double-minimum region occurs at values of x_0 where the fluctuation determinant vanishes due to the appearance of a caustic, thus leading to a singularity in the integrand of Eq. (2.3). This is not a disaster, however, as this singularity is integrable. (Such a singularity is an artifact of the semiclassical approximation. It disappears in a more refined approximation [8,11–13], in which one includes higher order fluctuations in the direction(s) of function space where the instability sets in.) We shall exhibit the details of this calculation in a forthcoming publication [14].

To conclude, two remarks: (i) our results may be used to derive a semiclassically improved perturbation expansion, which will be presented in Section IV; (ii) the semiclassical partition function incorporates, in an approximate way, quantum effects that become more and more relevant with the increase of the thermal wavelength. At very low temperatures, however, the quadratic approximations inherent to the semiclassical approximation fail to capture the details of the potential, which are important in the regime of large thermal wavelengths. Thus, we expect our calculations to be a better approximation at high temperatures. Indeed, studying the $T = 0$ limit of $Z_{\rm sc}(\beta)$ for the anharmonic oscillator, one finds no corrections to the unperturbed ground state energy. Nevertheless, this can be corrected by using the semiclassically improved perturbation theory just mentioned.

III. THE SEMICLASSICAL PROPAGATOR

In the next section we will show that, in order to go beyond the quadratic approximation of the preceding section, it is necessary to derive the semiclassical propagator, defined as:

$$G_j(\eta_1,\eta_2;\tau_1,\tau_2) \equiv \int_{\eta(\tau_1)=\eta_1}^{\eta(\tau_2)=\eta_2} [D\eta(\tau)]\, e^{-\Sigma_j/\hbar} \,, \tag{3.1}$$

$$\Sigma_j \equiv \frac{1}{2}\int_{\tau_1}^{\tau_2} d\tau \left\{ M\left(\frac{d\eta}{d\tau}\right)^2 + V''[x_j(\tau)]\,\eta^2 \right\} \,. \tag{3.2}$$

Σ_j involves the fluctuation operator, $\hat{F}_j$, which corresponds to the second functional derivative of the action around the classical trajectory, $x_j(\tau)$.

Formula (3.1) is the path-integral expression for the Euclidean time evolution operator, $\hat{\rho}_j$, of the quantum-mechanical problem defined by

$$-\hbar\frac{\partial}{\partial\tau}\,\hat{\rho}_j(\tau,0) = \hat{H}_j(\tau)\,\hat{\rho}_j(\tau,0) \,, \tag{3.3}$$

$$\hat{H}_j(\tau) \equiv -\frac{\hbar^2}{2M}\frac{\partial^2}{\partial\eta^2} + \frac{1}{2}V''[x_j(\tau)]\,\eta^2 \,. \tag{3.4}$$

Indeed, the propagator is given by

$$G_j(\eta_1,\eta_2;\tau_1,\tau_2) = \langle\eta_2|\hat{\rho}_j(\tau_2,\tau_1)|\eta_1\rangle \,. \tag{3.5}$$

Thus, it is just a density matrix element, as suggested by equation (3.4).

As the integral in (3.1) is Gaussian ($\hat{H}_j$ is quadratic), it is completely determined in terms of the extremum, $\bar{\eta}_j(\tau)$, of $\Sigma_j[\eta(\tau)]$, which satisfies

$$-M\,\frac{d^2\bar{\eta}_j}{d\tau^2} + V''[x_j(\tau)]\,\bar{\eta}_j = 0\,, \tag{3.6}$$

with the boundary conditions

$$\bar{\eta}_j(\tau_1) = \eta_1 \quad \text{and} \quad \bar{\eta}_j(\tau_2) = \eta_2\,. \tag{3.7}$$

The semiclassical propagator is, then,

$$G_j(\eta_1,\eta_2;\tau_1,\tau_2) = G_j(0,0;\tau_1,\tau_2)\, e^{-\bar{\Sigma}_j/\hbar} \,, \tag{3.8}$$

with $\bar{\Sigma}_j \equiv \Sigma_j[\bar{\eta}_j(\tau)]$. Using equations (3.1), (3.6) and (3.7), we have

$$\bar{\Sigma}_j = \frac{M}{2}\left[\eta_2\dot{\bar{\eta}}_j(\tau_2) - \eta_1\dot{\bar{\eta}}_j(\tau_1)\right]. \tag{3.9}$$

The fluctuation determinant discussed in the previous section can be obtained as

$$\Delta_j^{-1/2}(x_0,\beta) = G_j(0,0;0,\beta\hbar) \,. \tag{3.10}$$

The extremum, $\bar{\eta}_j(\tau)$, will be the linear combination of two linearly independent solutions of equation (3.6), $a_j(\tau)$ and $b_j(\tau)$, which satisfies the boundary conditions (3.7):

$$\bar{\eta}_j(\tau) = \frac{\eta_1 b_{j2} - \eta_2 b_{j1}}{a_{j1}b_{j2} - a_{j2}b_{j1}}\,a_j(\tau) + \frac{\eta_2 a_{j1} - \eta_1 a_{j2}}{a_{j1}b_{j2} - a_{j2}b_{j1}}\,b_j(\tau) \,, \tag{3.11}$$

with $a_{ji} \equiv a_j(\tau_i)$ and $b_{ji} \equiv b_j(\tau_i)$. This allows us to compute $\bar{\Sigma}_j$. Introducing the functions

$$\mathcal{F}_{j1}(\tau) \equiv a_{j1} b_j(\tau) - a_j(\tau) b_{j1}\,, \tag{3.12}$$

$$\mathcal{F}_{j2}(\tau) \equiv a_{j2} b_j(\tau) - a_j(\tau) b_{j2}\,, \tag{3.13}$$

which satisfy $\mathcal{F}_{j1}(\tau_1) = 0$, $\mathcal{F}_{j2}(\tau_2) = 0$ and $\mathcal{F}_{j1}(\tau_2) = -\mathcal{F}_{j2}(\tau_1)$, and the Wronskian

$$W_j(\tau) \equiv a_j(\tau)\dot{b}_j(\tau) - \dot{a}_j(\tau) b_j(\tau)\,, \tag{3.14}$$

we may write

$$\bar{\Sigma}_j = \frac{M}{2} \sum_{a,b=1}^{2} s_{ab}^{(j)} \eta_a \eta_b\,, \tag{3.15}$$

where

$$s_{11}^{(j)} \equiv -\frac{\dot{\mathcal{F}}_{j2}(\tau_1)}{\mathcal{F}_{j2}(\tau_1)}\,, \quad s_{12}^{(j)} \equiv \frac{W_j(\tau_1)}{\mathcal{F}_{j2}(\tau_1)}\,, \quad s_{21}^{(j)} \equiv -\frac{W_j(\tau_2)}{\mathcal{F}_{j1}(\tau_2)}\,, \quad s_{22}^{(j)} \equiv \frac{\dot{\mathcal{F}}_{j1}(\tau_2)}{\mathcal{F}_{j1}(\tau_2)}\,. \tag{3.16}$$

Using equations (3.4), (3.3), (3.5) and (3.8), we obtain

$$\left[\frac{\partial}{\partial \tau_2} + \frac{1}{2}\frac{\dot{\mathcal{F}}_{j1}(\tau_2)}{\mathcal{F}_{j1}(\tau_2)}\right] G_j(0,0;\tau_1,\tau_2) = 0\,, \tag{3.17}$$

which leads to

$$G_j(0,0;\tau_1,\tau_2) = C_j(\tau_1)\,[\mathcal{F}_{j1}(\tau_2)]^{-1/2}. \tag{3.18}$$

As $\tau_2 \to \tau_1$, we must recover the free-particle result:

$$\lim_{\tau_2 \to \tau_1} G_j(0,0;\tau_1,\tau_2) = \left[\frac{M}{2\pi\hbar(\tau_2 - \tau_1)}\right]^{1/2} \tag{3.19}$$

Expanding $\mathcal{F}_{j1}(\tau_2)$ in equation (3.18) around τ_1, and using equation (3.19), we can determine $C_j(\tau_1)$. Finally:

$$G_j(0,0;\tau_1,\tau_2) = \left[\frac{M}{2\pi\hbar}\frac{\dot{\mathcal{F}}_{j1}(\tau_1)}{\mathcal{F}_{j1}(\tau_2)}\right]^{1/2}. \tag{3.20}$$

All that remains is to find the two linearly independent solutions of (3.6), $a_j(\tau)$ and $b_j(\tau)$. The arguments of section II allow us to restrict our attention to single turning point paths, although we will sketch how one should proceed in the most general case, at the end of this section.

It can be easily checked that $\dot{x}_j(\tau)$ satisfies equation (3.6), by simply differentiating the Euclidean classical equation of motion with respect to Euclidean time. Then:

$$a_j(\tau) = \dot{x}_j(\tau). \tag{3.21}$$

If we consider $\tau \leq \beta\hbar/2$, one can check that

$$c_j \equiv \dot{x}_j(\tau) \int_0^\tau \frac{dt}{\dot{x}_j^2(t)} \tag{3.22}$$

also satisfies equation (3.6), again thanks to the equation of motion satisfied by $\dot{x}_j(\tau)$. Therefore, it can be used as $b_j(\tau)$ for $\tau \leq \beta\hbar/2$. It can be shown that $c_\pm^j \equiv c_j(\beta\hbar/2)$ and $\dot{c}_\pm^j \equiv \dot{c}_j(\beta\hbar/2)$ are well-defined [14]. Clearly, these will be the values of b_j and $\dot{b}_j$ at $\beta\hbar/2$. In order to find our other solution, for $\tau > \beta\hbar/2$, we cannot use $c_j(\tau)$, which is ill-defined beyond $\beta\hbar/2$. However, we may use

$$\tilde{c}_j(\tau) \equiv \dot{x}_j(\tau) \int_{\beta\hbar}^\tau \frac{dt}{\dot{x}_j^2(t)} \,. \tag{3.23}$$

A linear combination of $a_j(\tau)$ and $\tilde{c}_j(\tau)$ may, then, be constructed whose value at $\beta\hbar/2$ and that of its derivative coincide with $b_j(\beta\hbar/2) \equiv c_j(\beta\hbar/2)$ and $\dot{b}_j(\beta\hbar/2) \equiv \dot{c}_j(\beta\hbar/2)$. These two conditions determine the linear combination and guarantee continuity. As a result, we may now define $b_j(\tau)$ for all values of τ:

$$b_j(\tau) = \begin{cases} \dot{x}_j(\tau) \int_0^\tau \frac{dt}{\dot{x}_j^2(t)} & \text{for } \tau \leq \beta\hbar/2, \\ \dot{x}_j(\tau) \int_{\beta\hbar}^\tau \frac{dt}{\dot{x}_j^2(t)} - 2c_\pm^j \dot{c}_\pm^j \dot{x}_j(\tau) & \text{for } \tau \geq \beta\hbar/2. \end{cases} \tag{3.24}$$

We note that both $a_j(\tau)$ and $b_j(\tau)$ can be completely expressed in terms of the potential and of the value of the (single) turning point. Also, for the general case of two turning points, we can use the above procedure to obtain a piecewise construction of $b_j(\tau)$. For the first piece, we trade $\beta\hbar/2$ for the $\tau^\star$ where the first turning point is visited. Then, $\beta\hbar$ will be traded for $2\tau^\star$. This will allow us to define $b_j(\tau)$ up to $2\tau^\star$. We may proceed in the same fashion to the next turning point and repeat the operation to account for the number of cycles involved.

Equation (2.8) was obtained from $G_j(0,0;0,\beta\hbar)$, for the general case. From the knowledge of $\bar{\eta}_j(\tau)$, we can write a final expression for $G_j(\eta_1,\eta_2;\tau_1,\tau_2)$:

$$G_j(\eta_1,\eta_2;\tau_1,\tau_2) = \frac{1}{\sqrt{2\pi\sigma_j^2}}\, e^{-\frac{1}{2\sigma_j^2}\left[A_{12}^j\eta_2^2 + A_{21}^j\eta_1^2 - 2\eta_1\eta_2\right]} \tag{3.25}$$

$$\sigma_j = \frac{\hbar}{M}\,\mathcal{F}_{j1}(\tau_2)\,, \tag{3.26}$$

$$A_{12}^j = \frac{a_j(\tau_1) + \dot{a}_j(\tau_2)\mathcal{F}_{j1}(\tau_2)}{a_j(\tau_2)}\,. \tag{3.27}$$

This will be the basis for the semiclassical expansion to be derived in our next section.

IV. THE SEMICLASSICAL EXPANSION

We are now in a position to go beyond the quadratic approximation. To do so, we expand the action around a classical trajectory, $x_j(\tau)$, to all orders. Letting $x(\tau) = x_j(\tau) + \eta(\tau)$, with $\eta(0) = \eta(\beta\hbar) = 0$, we obtain:

$$S[x(\tau)] = S[x_j(\tau)] + \frac{1}{2!}\int_0^{\beta\hbar} d\tau\, \eta(\tau)\, \hat{F}_j\, \eta(\tau) + \sum_{n=3}^{\infty} \frac{1}{n!}\int_0^{\beta\hbar} d\tau\, V^{(n)}[x_j(\tau)]\, \eta^n(\tau), \tag{4.1}$$

where $V^{(n)} \equiv d^n V/dx^n$, and the second term is the quadratic piece. Use was made of the fact that higher functional derivatives involve products of delta functions.

As we take $e^{-S/\hbar}$ and integrate over the deviations, $\eta(\tau)$, from the classical trajectory, we may expand the higher than quadratic terms in a power series. Defining:

$$\int_0^{\beta\hbar} d\tau\, \delta L_j \equiv \sum_{n=3}^{\infty} \frac{1}{n!}\int_0^{\beta\hbar} d\tau\, V^{(n)}[x_j(\tau)]\, \eta^n(\tau), \tag{4.2}$$

we may interchange the integral over τ above with the sums over deviations from the classical path. This has the effect of breaking up the path integral into pieces that go from zero to the various times corresponding to multiple insertions of δL_j and, finally, to $\beta\hbar$. The result of doing the path integral in each piece yields the semiclassical propagator at different time intervals. The expression for the partition function becomes:

$$\begin{aligned} Z(\beta) = \int_{-\infty}^{\infty} dx_0 \sum_{j=1}^{N(x_0,\beta)} e^{-S_j/\hbar}\, [&G_j(0,0;0,\beta\hbar) \\ &-\frac{1}{\hbar}\int_0^{\beta\hbar} d\tau_1 \int_{-\infty}^{\infty} d\eta_1\, G_j(0,\eta_1;0,\tau_1)\, \delta L_j(\tau_1,\eta_1)\, G_j(\eta_1,0;\tau_1,\beta\hbar) \\ &+\frac{1}{2\hbar^2}\int_0^{\beta\hbar} d\tau_2 \int_{-\infty}^{\infty} d\eta_2 \int_0^{\tau_2} d\tau_1 \int_{-\infty}^{\infty} d\eta_1\, G_j(0,\eta_1;0,\tau_1)\, \delta L_j(\tau_1,\eta_1) \\ &\times G_j(\eta_1,\eta_2;\tau_1,\tau_2)\, \delta L_j(\tau_2,\eta_2)\, G_j(\eta_2,0;\tau_2,\beta\hbar)] + O(3) \end{aligned} \tag{4.3}$$

Clearly, the Gaussian dependence of the semiclassical propagator on the η variables, together with the fact that δL_j only involves powers of η, allows the integrals over η to be easily performed. As for the τ dependence, it is completely known, although the integrals involved may not be done analytically. The integrals over τ can, alternatively, be transformed into integrals over x (the classical position). We should note that the first term in (4.3) is just the fluctuation determinant and that each individual term in the series corresponds to an infinite sum of diagrams in ordinary perturbation theory, plus additional terms which depend on the classical solution.

In order to illustrate the usefulness of the expansion, let us outline some of its consequences in the case of the single-well quartic anharmonic oscillator, $V(x) = \frac{1}{2}m\omega^2 x^2 + \frac{\lambda}{4}x^4$, already discussed in section II. If we define a dimensionless coupling $g \equiv \lambda\hbar/2m^2\omega^3$, the first order correction in the expansion, i.e., the second term in the bracket of equation (4.3), may be written as $-3g\, G_j(0,0;0,\beta\hbar)\, I_j(\beta,g)$, where I_j is a dimensionless integral:

$$I_j \equiv \frac{\omega^3}{(2c_\pm^j \dot{c}_\pm^j)^2}\int_0^{\beta\hbar} d\tau\, \left[b_j^4(\tau) + 4c_\pm^j \dot{c}_\pm^j b_j^3(\tau) a_j(\tau) + (2c_\pm^j \dot{c}_\pm^j)^2 b_j^2(\tau) a_j^2(\tau)\right] \tag{4.4}$$

The functions $a_j(\tau)$ and $b_j(\tau)$ can be expressed in terms of Jacobian elliptic functions and elliptic integrals [14] which we shall not write down. All we want to emphasize is that $I_j(\beta,g)$ can be expanded in a power series in g, just as $G_j(0,0;0,\beta\hbar)$. In ordinary perturbation

theory, the first order term is of order g, and goes at most as β, for large β. An n^{th} order term will go like $g^n\beta^n$ (subleading corrections in β are present). Here, in first order, we have a whole series in g times β. Thus, if we remember that the *exact* ground state $E_0(g)$ is the only state to contribute at large β:

$$Z(\beta) \stackrel{\beta\to\infty}{\longrightarrow} e^{-\beta E_0(g)} = e^{-\frac{\beta\hbar\omega}{2}} \left\{ 1 - \beta \left[E_0(g) - \frac{\hbar\omega}{2} \right] + O(\beta^2) \right\}, \tag{4.5}$$

we see that we obtain a nonperturbative estimate for $E_0(g)$, while perturbation theory would only give us an order g correction.

In order to compute correlation functions, one might introduce an external current, $j(\tau)$, coupled to the variable, $x(\tau)$, and use the knowledge of the semiclassical propagator to integrate the linear plus quadratic piece of the action to derive a functional of $j(\tau)$, to be used in the expansion in the standard way [15].

V. CONCLUSIONS AND OUTLOOK

The methods developed in the preceding sections allow us to deal with problems in one-dimensional Quantum Statistical Mechanics by means of a semiclassical expansion which is fully calculable and yields nonperturbative results.

Problems in higher-dimensional Quantum Statistical Mechanics with potentials that have spherical symmetry may be reduced, by means of partial-wave decompositions, to one-dimensional problems wherein our methods could be applied.

Furthermore, in finite temperature Field Theory, where the point x_0 of our previous treatment is to be replaced with the (static) field configuration, $\phi(\vec{x})$, we already see the need to consider extrema which must depend on τ, the Euclidean time, as we lower the temperature. Catastrophes will certainly occur, forcing us to rethink commonly used approximations that use constant field configurations as backgrounds to derive effective potentials. Here, again, under very special circumstances, one might hope that the methods developed so far may shed some light into the intrincacies of nonperturbative phenomena.

ACKNOWLEDGMENTS

This work was partially supported by CNPq, FUJB/UFRJ and CLAF. It is a pleasure to thank Eduardo Fraga and Sergio Jorás for help with the manuscript, as well as for comments and suggestions. Special thanks to the organizers of the La Plata meeting for their kind hospitality.

REFERENCES

[1] C. A. A. de Carvalho and R. M. Cavalcanti, Braz. J. Phys. **27**, 373 (1997).

[2] J. Zinn-Justin, *Quantum Field Theory and Critical Phenomena* (Oxford University Press, Oxford, 1993).

[3] D. Boyanovsky, R. Willey and R. Holman, Nucl. Phys. B **376**, 599 (1992).

[4] R. P. Feynman and A. R. Hibbs, *Quantum Mechanics and Path Integrals* (McGraw-Hill, New York, 1965).

[5] R. P. Feynman, *Statistical Mechanics* (Benjamin, Reading, MA, 1972).

[6] I. S. Gradshteyn and I.M. Ryzhik, *Table of Integrals, Series and Products* (Academic Press, New York, 1965).

[7] A partial examination of such a structure is found in: J. Ankerhold and H. Grabert, Physica A **188**, 568 (1992); Phys. Rev. E **52**, 4704 (1995); F. J. Weiper, J. Ankerhold and H. Grabert, Physica A **223**, 193 (1996).

[8] M. Berry, in *Physics of Defects*, Les Houches Session XXXV (1980), eds. R. Balian et al. (North-Holland, Amsterdam, 1981); M. V. Berry and C. Upstill, in *Progress in Optics XVIII*, ed. by E. Wolf (North-Holland, Amsterdam, 1980).

[9] P. T. Saunders, *An Introduction to Catastrophe Theory* (Cambridge University Press, Cambridge, 1980); R. Thom, *Structural Stability and Morphogenesis* (Benjamin, Reading, MA, 1975); T. Poston and I. N. Stewart, *Catastrophe Theory and its Applications* (Pitman, London, 1978); E. C. Zeeman, *Catastrophe Theory: Selected Papers 1972-1977* (Addison-Wesley, Reading, MA, 1977).

[10] This is an example of a sigma-decomposition. See, for example, M. Peixoto and R. Thom, C. R. Acad. Sc. Paris I, **303**, 629 and 693 (1986); **307**, 197 (1988) (Erratum); M. M. Peixoto and A. R. Silva, An. Acad. Bras. Ci. **62** (4), 321 (1990); M. M. Peixoto and A. R. Silva, preprint (1995).

[11] G. Dangelmayr and W. Veit, Ann. Phys. (NY) **118**, 108 (1979).

[12] L. S. Schulman, *Techniques and Applications of Path Integration* (Wiley, New York, 1981).

[13] U. Weiss, *Quantum Dissipative Systems* (World Scientific, Singapore, 1993).

[14] C. A. A. de Carvalho, R. M. Cavalcanti and S. E. Jorás, in preparation.

[15] D. J. Amit, *Field Theory, the Renormalization Group, and Critical Phenomena* (World Scientific, Singapore, 1984).

Figure Captions:

Figure 1: (a) Classical paths at x_m for $\beta < \pi/\hbar\omega_m$ (1) and $\beta > \pi/\hbar\omega_m$ (2 and 3); (b) Sketch of how the extrema change along the unstable direction in function space.

Figure 2: (a) Classical paths at x_m for $\beta < \beta_c$ (1), $\beta = \beta_c$ (1 and 2&3) and $\beta > \beta_c$ (1,2 and 3), $\pi/\hbar\omega_m < \beta_c < 2\pi/\hbar\omega_m$; (b) Sketch of how the extrema change along the unstable direction in function space.

Figure 3: Bifurcation set for the cusp; pattern of extrema shown schematically.

Figure 4: Evolution of the classical action as β changes. (a) $0 \leq \beta < \pi/\hbar\omega_m$; (b) $\pi/\hbar\omega_m < \beta < 2\pi/\hbar\omega_m$; (c) $2\pi/\hbar\omega_m < \beta < 3\pi/\hbar\omega_m$.

Figure 5: Partition of control space into p-solution regions ($p = 1, 3, 5, 7, \ldots$).

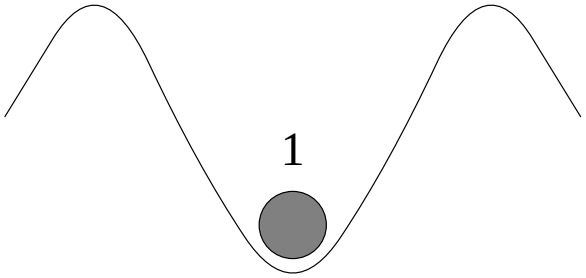

$$\beta\hbar < \frac{\pi}{\omega_m}$$

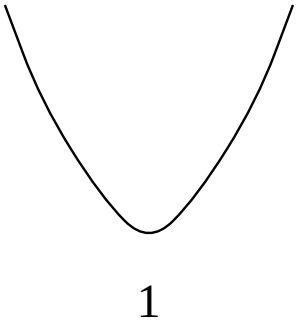

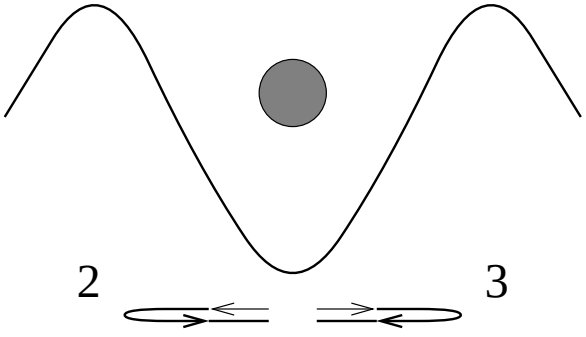

(a)

$$\beta\hbar > \frac{\pi}{\omega_m}$$

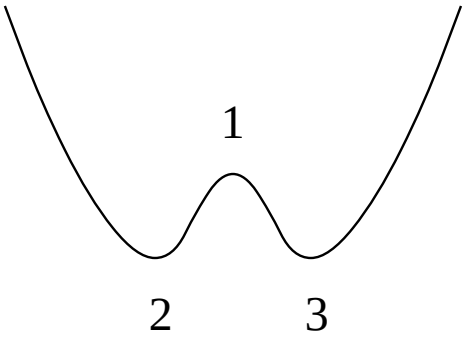

(b)

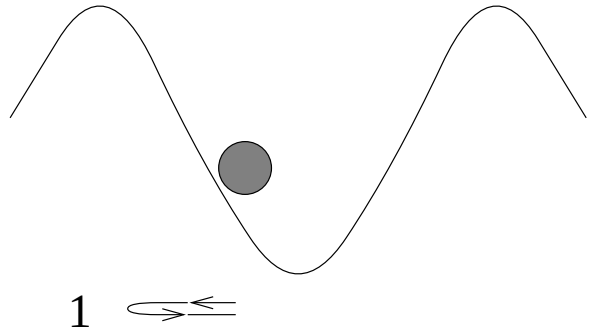

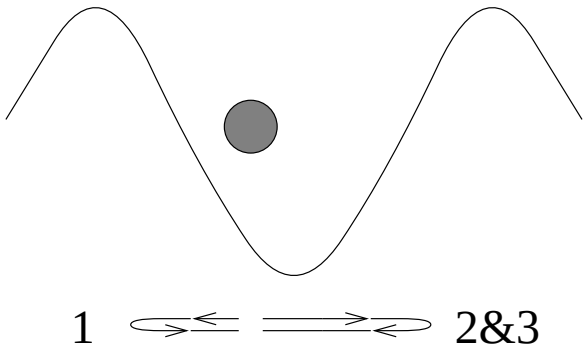

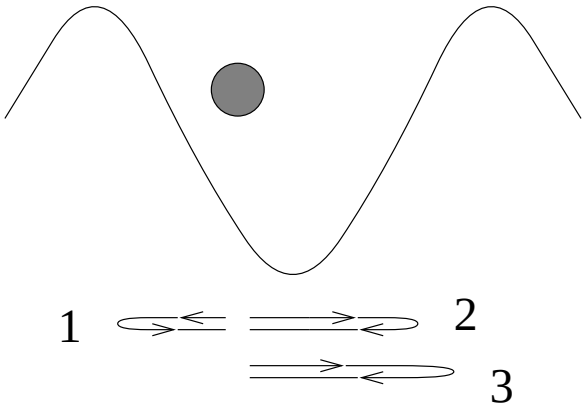

(a)

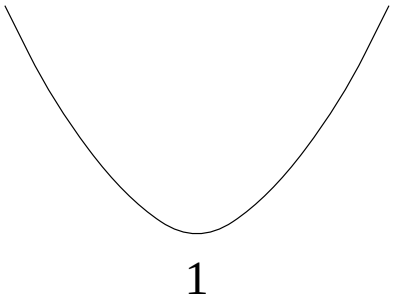

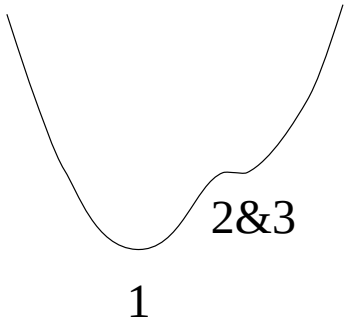

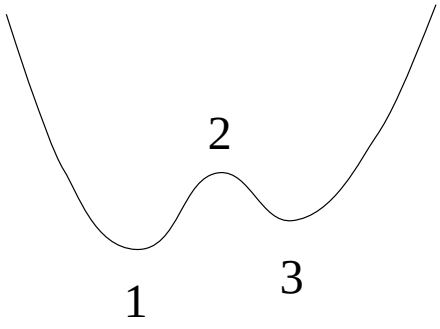

(b)

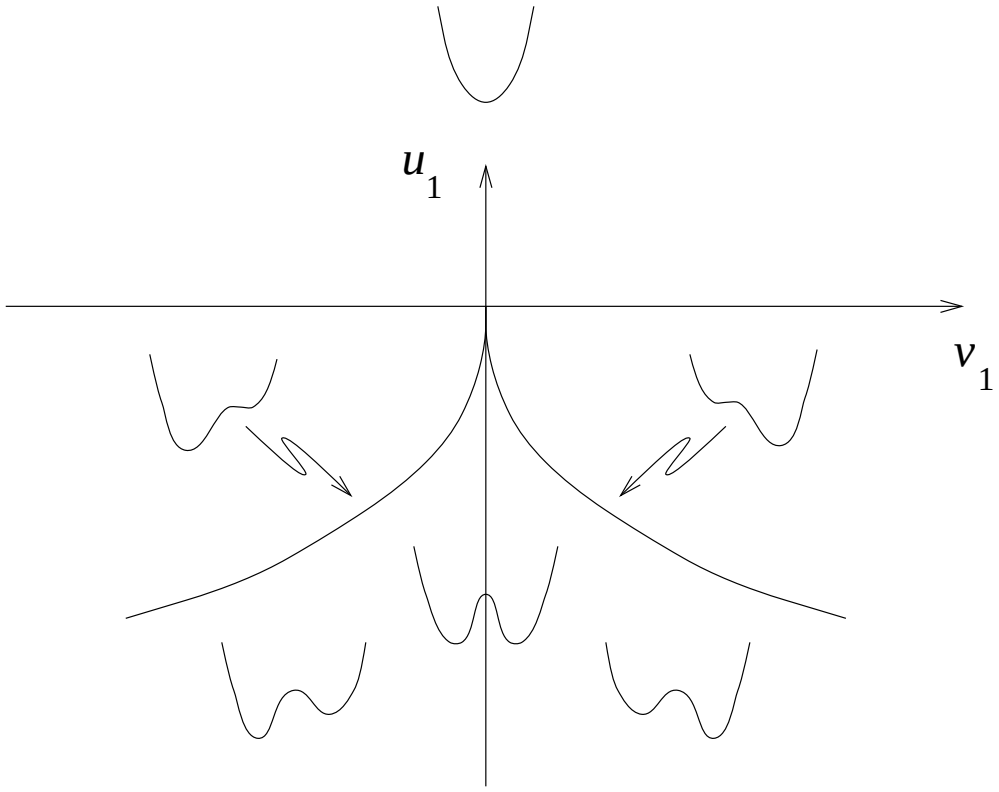
u_1
v_1

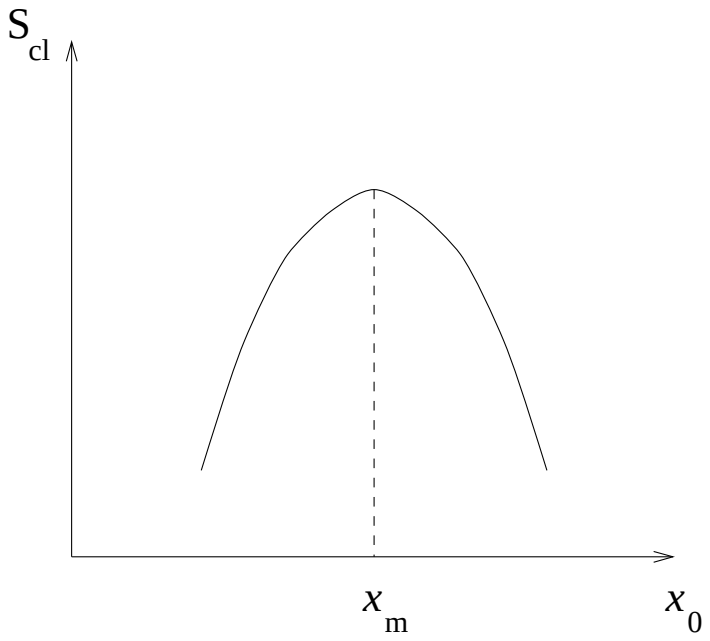

(a)

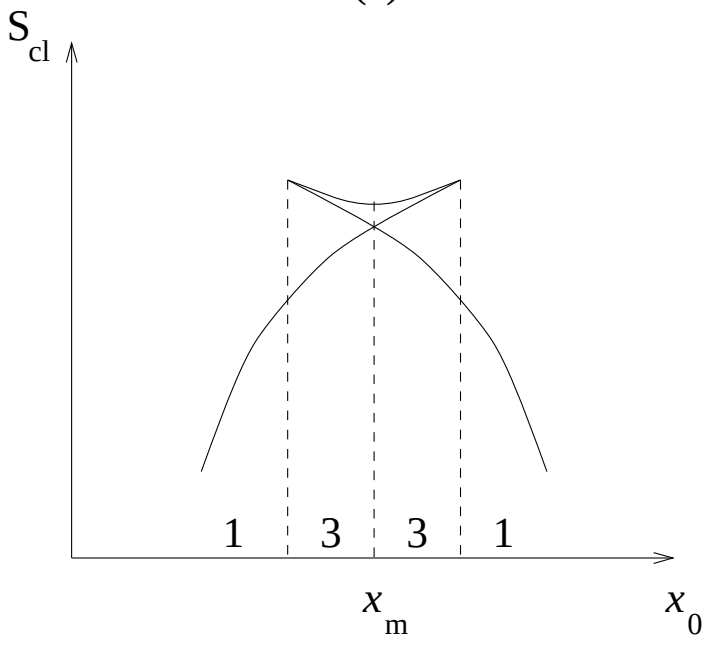

(b)

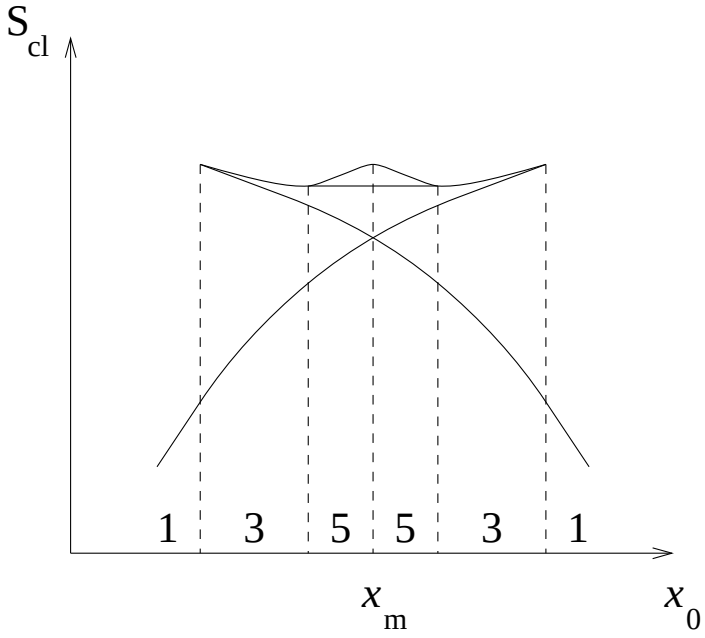

(c)

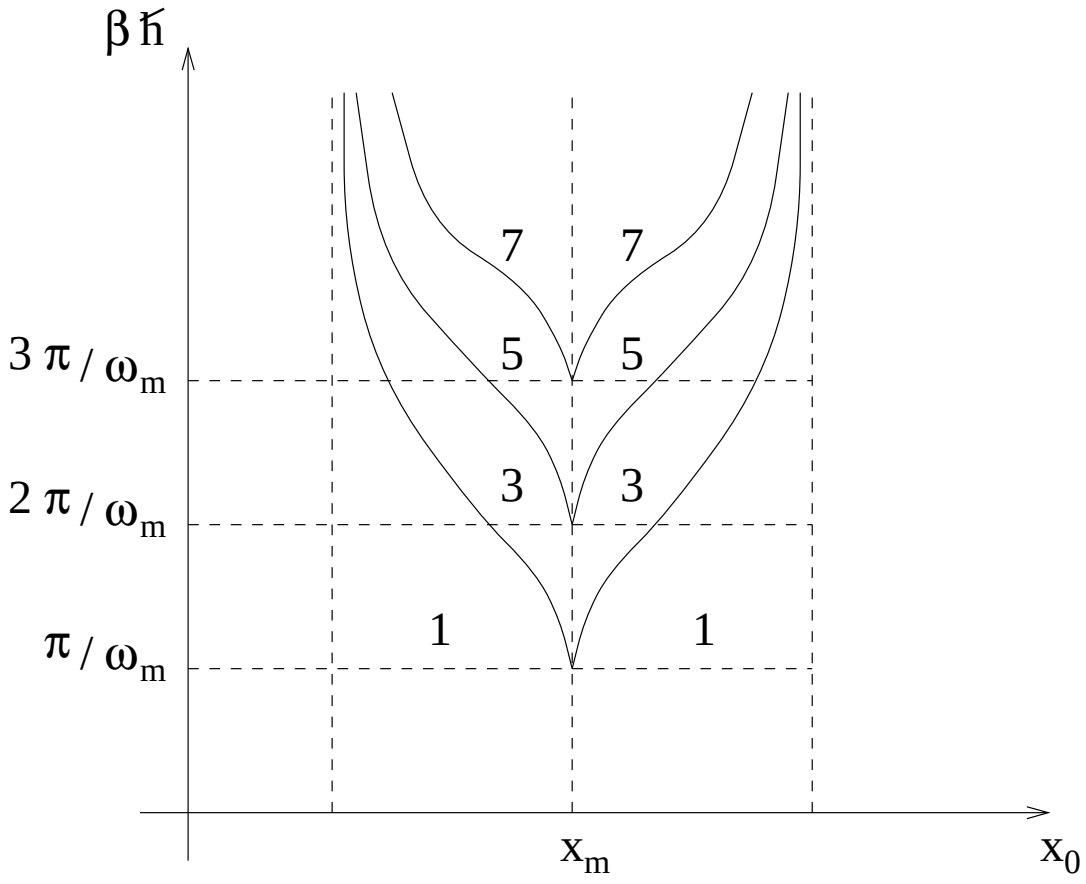
β ħ
3 π / ω_m
2 π / ω_m
π / ω_m
7
7
5
5
3
3
1
1
x_m
x_0